Article

Effect of Water Level Fluctuation on Riverbank Stability at the Estuary Area of Muaro Kualo Segment, Muara Bangkahulu River in Bengkulu, Indonesia

Lindung Zalbuin Mase[1,a,*], Khairul Amri[1,b], Muhammad Farid[2,c], Fandi Rahmat[2,d], Muharram Nur Fikri[2,e], Jihan Saputra[2,f], and Suched Likitlersuang[3,g]

1 Department of Civil Engineering, Faculty of Engineering, University of Bengkulu, Bengkulu, Indonesia
2 Department of Geophysics, Faculty of Mathematics and Natural Sciences, University of Bengkulu, Bengkulu, Indonesia
3 Centre of Excellence in Geotechnical and Geoenvironmental Engineering, Department of Civil Engineering, Faculty of Engineering, Chulalongkorn University, Bangkok, Thailand
E-mail: [a,*]lmase@unib.ac.id (Corresponding author), [b]khairulftunib@yahoo.co.id, [c]mfarid@unib.ac.id, [d]fandirahmat831@gmail.com, [e]muharramn.fikri@gmail.com, [f]saputrajihan27@gmail.com, [g]fceslk@eng.chula.ac.th

Abstract. The paper presents an investigation of riverbank stability at the estuary area of Muaro Kualo Segment, Muara Bangkahulu River in Bengkulu, Indonesia. This area had experienced slope failures along the riverbank during the Bengkulu flood in 2019. This study is initiated by conducting a geotechnical survey to observe site condition. During the survey, slope geometry measurement and soil sampling are performed. The laboratory tests are performed to collect physical and engineering soils properties. The rainfall intensity during period of 2011-2020 is also collected to observe normal and critical river water level. The finite element method is employed to analyse the slope stability analysis under the normal and critical river water level conditions. The results showed that the slope failure is generally initiated at the slope toe. Because of the river water level, factor of safety of slope along the estuary is less than the minimum criteria for the stable slope. It indicates that slope failure is very possible to occur. Implementation of sheet pile is conducted to reduce the slope failure potential. The results showed that the use of sheet pile is relevant to improve slope stability in the study area.

Keywords: Estuary area, slope failures, rainfall intensity, finite element method, flood.

1. Introduction

In general, Bengkulu Province is known as a province in Indonesia that is very vulnerable to undergo seismic hazards [1]. Bengkulu Province itself is located at the coastal area of Sumatra Island that is directly facing Indian Ocean. Within last 10 years, the climate change effects had resulted several impacts to the environment in several areas around Indian Ocean, including Bengkulu City, the capital city of Bengkulu Province [2]. It is proved by many huge floods occurred within last 10 years. Recently, in the end of April 2019, a very heavy rainfall intensity had triggered so many inundations in Bengkulu City [3] and landslides in the mountainous area [4]. The impact of flood during April 2019 was not only reflected by massive inundated areas in Bengkulu City, but also slope failures along riverbanks.

One of the areas that underwent the impact of slope failures during the flood was the estuary area of Muara Bangkahulu River (Fig. 1). Muara Bangkahulu River is the main river in Bengkulu City that has upstream area in the mountainous area, Central Bengkulu Regency. The main cause of flood in 2019 was due to the overflow of the Muara Bangkahulu River during the long period of heavy rainfall in the end of April 2019 [4]. The estuary area of Muara Bangkahulu River is very important for local people in Bengkulu City. This area has the traditional port that supports local activity. The traditional port services for the local transportation, the temporary place for ships maintenance, and the tourism area in Bengkulu City. During the flood in 2019, the services were dormant due to the increase of river level and slope failures along the riverbank. The increase of river level itself is suspected as the main factor triggering slope failures along the estuary area. In line with the flood impact, it is important to study the effect of water level fluctuation to slope stability at the estuary area, Muaro Kualo, Bengkulu City.

In geotechnical engineering, the implementation of stability countermeasure is important issue in slope countermeasure. Several researchers, such as Komolvilas et al. [5] and Jamsawang et al. [6] mentioned that stability countermeasure is important as a component to monitor the progress of field construction for sloping ground that can be a recommendation to improve the slope stability. Leknoi and Likitlersuang [7] also mentioned that the understanding on slope stability countermeasure could be good practice and lesson learned in improving the landslide hazard mitigation.

For slope stability investigation, several studies had been conducted to investigate the effect of river water level in other areas. Duong et al. [8] conducted a study of slope stability under flooding condition in the riverbank of Red River, Vietnam. Thi and Minh [9] conducted a study of the effect of rainfall intensity and hydraulic conductivity to stability of Red River riverbank in Vietnam. Based on their study, Thi and Minh [9] concluded that during the high rainfall intensity, the highly-saturation process occurred in soil mass. This condition leads into the increase of slope failure potential. Liang et al. [10] observed the effect of river water level fluctuation to slope stability of riverbank in Long Island, Australia. Their study showed that the rapid decrease of river water or rapid drawdown can result in slope failure. Liang et al. [10] also mentioned that river fluctuation tends to be more dominant rather than climate change effect in influencing slope failure. Extreme rainfall events which trigger the increase of river water level are also likely to trigger riverbank collapse. Udomchai et al. [11] performed an investigation to the collapse of riverbank protection in Saraburi, Thailand. Udomchai et al. [11] mentioned that the main factor triggering the collapse of riverbank is seepage during the rainy season. Udomchai et al. [11] also suggested that the extreme river stream was likely to scour riverbank. This scouring zone became a seepage path. The accumulation of water infiltration furthermore reduced shear strength and then it collapsed. In general, the results of those studies had concluded that the riverbank failures are generally caused by the effect of fluctuation river water level during floods.

In line with the field evidence of riverbank slope failure during the flood in 2019 in Bengkulu City, a study of slope stability analysis considering the fluctuation of river water is conducted. Site investigation and laboratory test are performed to obtain the physical properties of soils at the riverbank of Muara Bangkahulu River in the estuary area. The finite element simulation is conducted to observe soil behaviour and slope stability at the riverbank. Several outcomes, such as factor of safety (FS) and total displacement are observed. To depict the spatial mapping of slope vulnerability in the study area, the mapping method using the combination of Krigging and Gridding interpolations is used. In general, the results of this study could lead the local government to consider slope countermeasure in the study area.

2. Material and Method

2.1. Study Area and Soil Properties

This study is focused on the estuary area of Muara Bangkahulu River, called Muaro Kualo Area (Fig. 1). In the past, this area is known as the old-city of Bengkulu because this area was the first developed zone in the past. Nowadays, this area is still functioned as a traditional port in Bengkulu City. During the Bengkulu flood in 2019, riverbank failures were found. The normal activities such as ship reparation, tourism, and daily necessities trading are disturbed due to the riverbank failures. The increase of river water level during the flood has been suspected as the main cause of riverbank failures in the study area. In this study, 10 slopes located along the estuary area are studied. The slopes are indicated by red arrows namely MK-1 to MK-10, as shown in Fig. 2. In general, the slope height is observed to vary from 4 to 6 m high, and the slope width is observed to vary from 5 to 13.5 m with the average river water level of about 2.88 m. At those sites, the

handboring test is conducted to obtain undisturbed sampling. The test is conducted up to 2 m depth. The undisturbed sampling is further investigated in the laboratory.

Several physical properties and engineering properties are investigated in geotechnical laboratory. Table 1 presents summary of laboratory test results for soils at the study area. Based on the laboratory test, it can be observed that soil type at the study area, especially at the investigated cross sections, is classified as silty sand (SM). The unit weights of soils under bulk, dry, and saturated conditions are observed to vary from 14.92 to 16.27 kN/m³; 9.65 to 11.21 kN/m³; and 15.36 to 16.73 kN/m³, respectively. The sandy soils are generally having high degree of saturation, i.e., about 78% to 94%. It indicates that the soil is relatively wet. The parameters of consistency show that plasticity index range from 5.58 to 12.71%. To classify the soil type, Unified Soil Classification System (USCS) [13] is used. Based on Table 1, the soil consistency shows that silt contain also includes in the soil. The direct shear test is also conducted to obtain shear strength parameters. Several studies [3, 4, and 14] shows that soil strength of sandy soil tends to be dominated by internal friction angle. For silty and clayey sands, another parameter called soil cohesion also plays role to determine shear strength. In Table 1, it can be observed that soil cohesion is observed to vary from 3.53 to 5.30 kN/m² and internal friction angle is observed to vary from 28.10 to 29.47°. The elastic modulus and Poisson's ratio are determined based Bowles' [15] recommendation. Soil properties and slope geometry are used as the parameters for finite element simulation in analysing slope stability at the study area.

2.2. Hydrological Analysis

The main goal of this study is to observe slope vulnerability based on the effect of river water level. Therefore, in this study, the river water level increase is estimated from the effect of rainfall during last 10 years. To determine the river water level increase, the rational discharge analysis is conducted. The rational discharge equation is expressed in this following equation,

$$Q_{rat} = 0.278 \cdot C \cdot I \cdot A \qquad (1)$$

In Eq. (1), Q_{rat} is the rational discharge, C is coefficient of surface runoff, I is rainfall intensity, and A is the drainage.

In general, the discharge is also able to be estimated by using the correlation between cross-sectional area and stream velocity as expressed in Eq. (2). For Eq. (2), Q is the normal discharge, A_c is cross-sectional area of river and v is the velocity of river stream. Based on Eq. (2), it can be seen that discharge can be calculated by using velocity and the cross-sectional area of river.

$$Q_n = A_c \cdot v \qquad (2)$$

Fig. 1. Layout of study area (basic map modified from Google Earth [12]).

Figure 3 presents the illustration of cross-sectional area of a river. It can be observed w_{n1} and w_{n2} are the parallel sides of cross-section for a river under normal condition, whereas h is the river water height under normal condition. Once flood occurred, rational discharge could contribute the river water flow. Therefore, in Fig. 3, there is additional height of river water due to the flood (h_f). As a result, a maximum parallel side due to the flood can be assigned as w_f. In line with both Eq. (1) and (2), it is simply applicable to estimate the increase of river water height by using both equations. The increase of river water level can be predicted by both equations that are combined to determine the increase of river water level as expressed in Eq. (3) to (5),

$$Q_{total} = Q_{rat} + Q_n \qquad (3)$$

$$Q_{total} = (0.278 \cdot C \cdot I \cdot A) + \left(\frac{1}{2} (w_{n1} + w_{n2}) \cdot h_n \cdot v_n \right) \qquad (4)$$

$$Q_{total} = \left(\frac{1}{2} (w_{n2} + w_f) \cdot h_f \cdot v_f \right) \qquad (5)$$

In Eq. (3) to (5), total discharge (Q_{total}) is estimated based on the summation of rational discharge (Q_{rat}) and normal discharge (Q_n). It should be noted that the parameter of river flow velocity (v_n) and flood flow velocity (v_f) should be known to estimate Q_n and Q_{total}. Furthermore, by combining Eq. (4) and (5), the height of river water level can be estimated as expressed by this following equation,

$$h_f = \frac{2 \cdot Q_{total}}{(w_{n2} + w_f) \cdot v_f} \qquad (6)$$

2.3. Methodology

In general, this study is performed based on the combination between experimental study and numerical analysis. Both experiment and numerical analysis are performed by following the research flowchart presented in Fig. 4. First, this study is conducted based on the last huge-floods in 2019 that had resulted in the impact to estuary area of Muara Bangkahulu River. The slope failures along the riverbank are also linked with the recent flood event occurring in Bengkulu City. Afterward, the next step is to conduct the literature reviews for supporting this study. Several literatures, such as the characteristic of Muara Bangkahulu downstream area [14], flood event in Bengkulu City [3], factors influencing slope failure [16], and finite element method for slope stability analysis [3, 4] are studied.
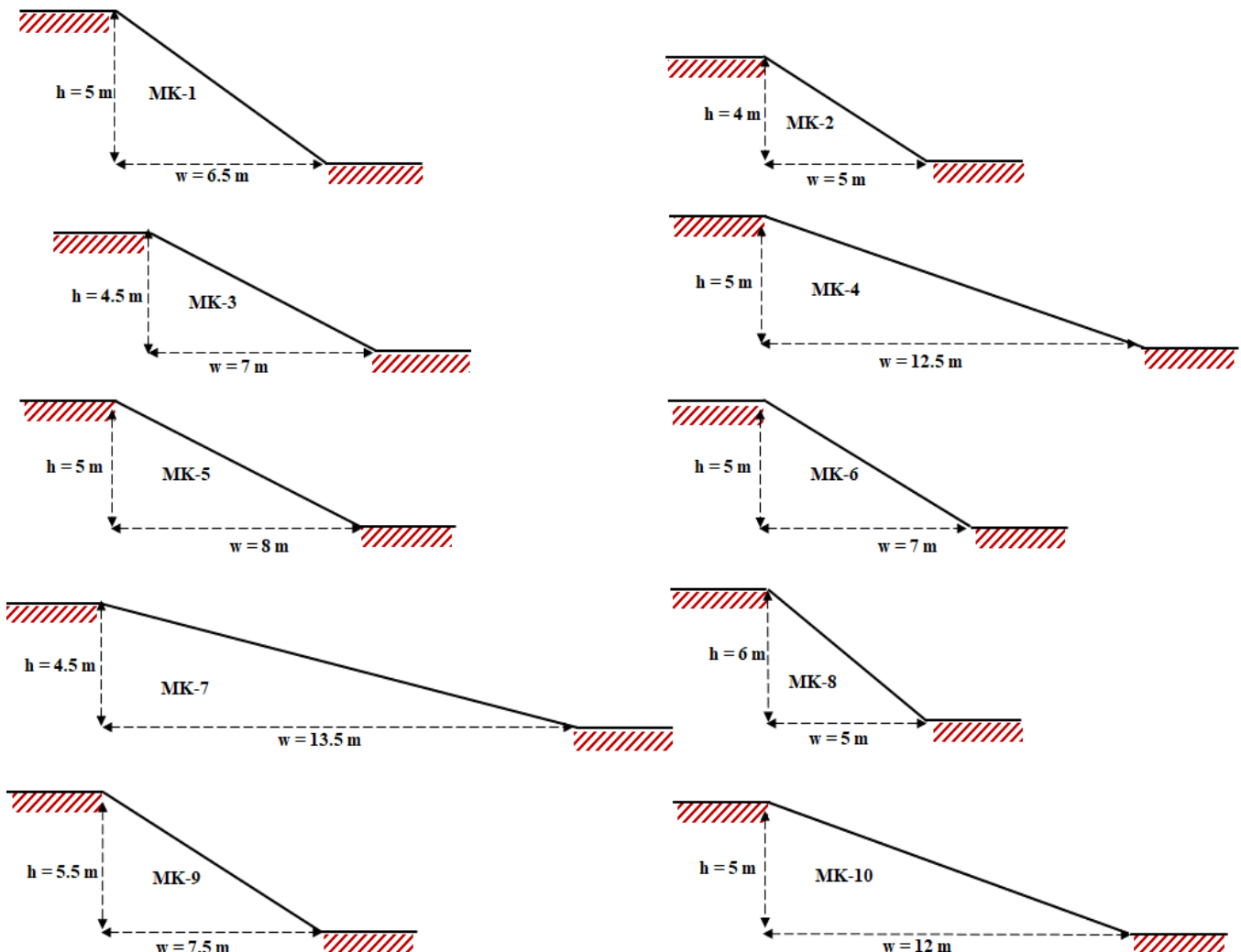
Fig. 2. Slope cross-sections.

Table 1. Summary of laboratory test results.

Soil Properties	Notation	Unit	Cross section at Muara Kualo Segment (MK)									
			1	2	3	4	5	6	7	8	9	10
Soil Classification	USCS	-	SM	SM	SM	SM	SM	SM	SM	SM	SM	SM
Unit Weight												
*Bulk unit weight	γ_b	kN/m³	15.25	16.27	15.95	14.99	16.09	15.26	14.92	15.82	15.76	14.57
*Dry unit weight	γ_d	kN/m³	9.812	11.21	10.76	9.65	11.13	10.08	10.54	10.88	10.45	10.44
*Saturated unit weight	γ_{sat}	kN/m³	15.72	16.48	16.69	15.36	16.49	16.04	16.73	16.22	16.67	16.54
Moisture content	w	%	55.43	45.18	48.25	55.39	44.57	51.41	41.59	45.41	50.84	39.53
Specific gravity	G_s	-	2.76	2.78	2.60	2.89	2.77	2.69	2.53	2.82	2.53	2.58
Void ratio	e	-	1.76	1.43	1.37	1.94	1.44	1.62	1.36	1.54	1.38	1.42
Degree of saturation	S	%	86.96	87.61	91.49	82.53	85.63	85.42	77.62	82.99	93.52	71.64
Consistency limits												
*Liquid limit	LL	%	43.17	42.65	41.97	38.60	40.46	40.82	43.98	39.93	41.30	42.58
*Plastic limit	PL	%	33.13	29.94	36.39	30.95	33.13	33.13	36.39	33.13	33.13	36.39
*Plasticity Index	PI	%	10.04	12.71	5.58	7.65	7.33	7.69	7.59	6.80	8.17	6.19
Soil cohesion	c	kN/m²	4.81	3.55	4.53	5.16	4.85	4.09	4.03	3.53	5.30	3.57
Internal friction angle	ϕ	°	28.74	28.77	29.79	28.79	28.96	28.74	28.10	29.47	28.60	28.63
Coefficient of permeability	k	cm/hour	0.47	0.51	0.52	0.48	0.50	0.51	0.48	0.51	0.47	0.51
Elastic Modulus	E	kN/m²	10,326	10,388	12,164	10,414	10,711	10,326	9,215	11,604	10,081	10,143
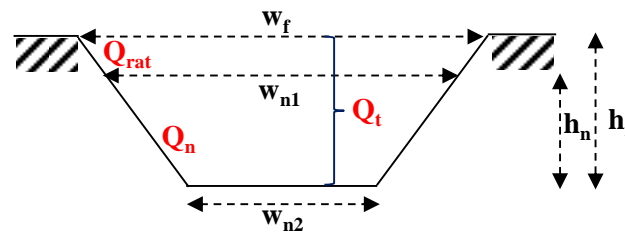
Note
w_f : a maximum parallel side due to flood
w_{n1} and w_{n2} : parallel side of cross-section for river under normal condition
h_n : height of river water level under normal condition
h_f : total height of river water level due to flood (critical condition)
Q_{rat} : rational discharge
Q_n : normal discharge
Q_{total} : total discharge

Fig. 3. The illustration of discharge and cross-sectional area during normal and critical condition.

The data collection is then conducted in this study. There are two types of data collected, i.e., primary data and secondary data. Several information, such as geometry of slope, physical and engineering properties of soil, river water level under normal condition are categorised as the primary data. The intensity of rainfall from 2000 to 2020, maps of topography and land-use are categorised as secondary data for this study. After data collection, the data recapitulation is performed. To examine the reliability of collected data, the data validation is also performed. In this study, the concern on soil properties is focused by observing the characteristics of soils. If the data collection has not completed, the step of data collection would have been re-performed. Otherwise, if the data has been completed, the next step, i.e., the analysis of maximum discharge would have been conducted. Furthermore, the rainfall intensity is analysed to estimate the maximum discharge. Next, the maximum discharge along the study area is used to estimate the river water level increase. The increase of river water level due to the maximum discharge is noted as the critical ground water level that can describe the maximum increment of river water level due to the flood.

After the prediction of critical river water level has been known, the next step is to perform slope stability analysis for slope along riverbank of Muara Bangkahulu

River. In this study, a finite element method from Brinkgreve et al. [17] is employed. Several researchers [18-20] mentioned that the use of finite element method in engineering practice is very recommended. For the soil model parameter, a common model parameter called Mohr-Coulomb model is used. The implementation of finite element method has been introduced by several researchers in some geotechnical problems, such as slope stability analysis [4], bearing capacity of strip footing [21], deep excavation [22], and tunnelling [23]. Several researchers, such as Matsui and San [24], Dawson et al. [25], and Zhang et al. [26] confirmed that the use of finite element simulation under method of shear strength reduction (ϕ and c reduction) is relevant in the implementation of slope stability. Mase et al. [27] mentioned that shear-strength reduction is one of appropriate parameter to observe stability of soils. the stability of Dyson and Tolooiyan [28] mentioned that shear strength reduction method is applicable to precisely estimate each optimised reduction stage during finite element simulation. The implementation of shear strength reduction is also reliable for slope stability cases, such as heterogeneous slope stability [29], reinforced slope stability [30] and rock slope stability [31]. Based on the implementation of shear strength reduction on finite element simulation, it is therefore appropriate to use shear strength reduction method to analyse slope stability

of the estuary area of Muara Bangkahulu River in Bengkulu City. Several studies conducted by Leelarungroj *et al.* [32], Chompoorat *et al.* [33], and Punnoi *et al.* [34] mentioned that soil shear strength is the important component to improve soil stability. Therefore, for checking stability, shear strength should be considered.

The input parameters used in this study are referring to soil properties listed in Table 1. The main objective of this study is to observe slope stability due to increase of river water level. Therefore, there are two conditions, which are simulated in this study. The first one is the slope stability simulation under the normal river water level and the second one is the slope stability simulation under the critical river water level. For the normal water level, the measurement on river water level is performed, whereas for critical river water level is estimated from the maximum discharge analysis. From the simulation, several important results, such as factor of safety (FS) against slope failure and displacement, are collected. FS less than 1.5 indicates that the slope is vulnerable to failure, whereas FS equal to 1.5 indicates that the slope is under critical condition. The selection of FS of 1.5 as the threshold of slope stability is based on the study conducted by Stark and Ruffling [35] who mentioned that FS of 1.5 could be implemented for the area having the high environmental impact. Since the estuary area of Muara Bangkahulu River is categorised as the area with the high-vulnerable impact to the environmental

condition, the recommendation on this FS threshold can be applied. For FS more than 1.5, the slope could be categorised as stable slope which means that slope is not vulnerable to collapse [3].

In this study, failure criteria are implemented for simulation of finite element. The scenario of simulation is to build a riverbank slope model. Furthermore, the effect of river water is observed. There is no external load considered for simulation of natural slope stability because the simulation is conducted based on the natural condition. In terms of simulation stages, slope is first loaded by internal load. Afterwards, the shear strength reduction analysis is conducted to observe the failure mechanism.

Furthermore, the mapping of vulnerability level to the study area is conducted. In this study, Krigging and Gridding interpolating method [36] is employed to generate micro-zonation maps. In general, the results of this study could describe the effect of water level increase along Muara Bangkahulu downstream area, especially in Muara Kualo Segment. The results of this study could also deliver a recommendation to local government in considering the potential slope failure along the study area. The results could be also used as the basic guidelines to design slope countermeasure along the Muara Bangkahulu downstream area in order to avoid the significant slope failure during floods.
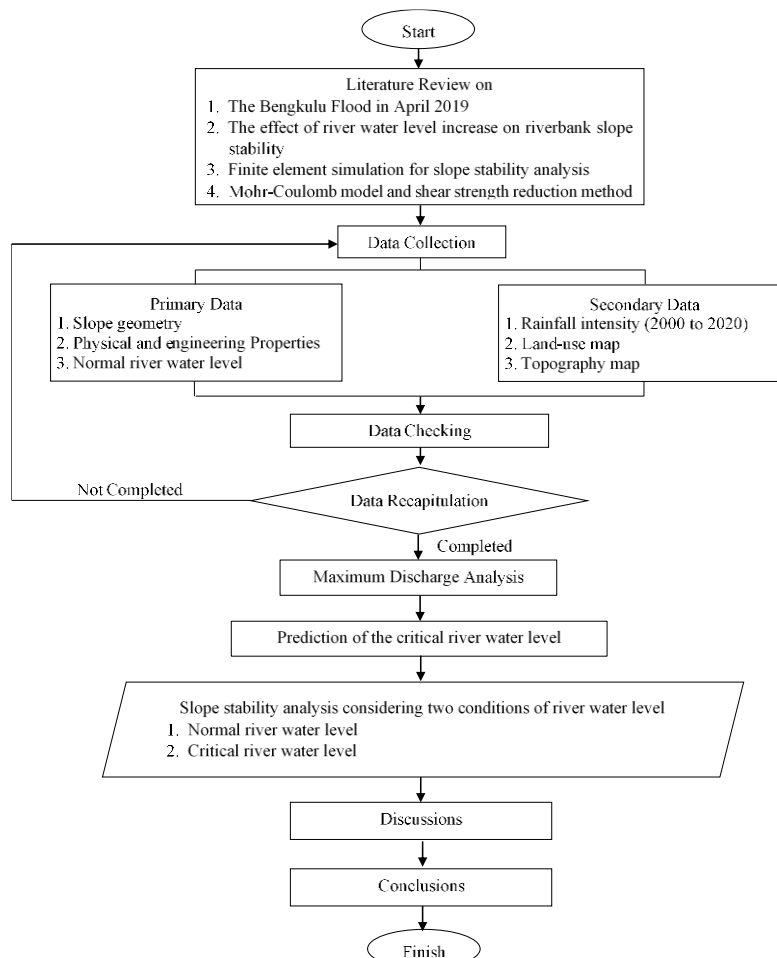
Fig. 4. Research framework.

3. Results and Discussion

3.1. Hydrological Analysis Results

In this study, the hydrological analysis is conducted based on the monthly rainfall intensity occurred in the period of 2011-2020. During this period, there is a huge event of the Bengkulu Flood in 2019. The monthly rainfall intensity from River Territory Office or RTO [37] is presented in Fig. 5. Based on Fig. 5, it can be seen that the minimum rainfall intensity within the period of 2011-2020 occurs in September with the rainfall intensity of 12.3 cm, whereas the maximum one occurs in November with the rainfall intensity of 23.85 cm. In general, the average rainfall intensity (I) within last 10 years is recorded of about 16.6 cm.

From the monthly rainfall intensity, the rational discharge analysis is conducted using Eq. (1). The analysis is employed to estimate the surface runoff resulted due to the rainfall in Bengkulu City. The results of rational discharge analysis are summarized in Table 2. It can be seen that the discharge on the study area is generally observed to vary from 269 to 314 m3/s. The study area is located at the edge of Bengkulu City. Based on recommendation from McCuen [38], C parameter can be assigned as 0.6. For section area, the segmented areas are grouped in to 5 regions as shown in Fig. 1 (shown by

blue dashed lines). The consideration in dividing the study area to be 5 regions is based on the zoning characteristics that consider the factors including topography, river meander, and so on.

Before calculating the total discharge, the normal discharge should be first estimated. In this study, Eq. (2) is used to obtain the normal discharge in the study area. Table 3 presents the summary of normal discharge under the existing condition in the study area. In Table 3, it can be observed that based on the field measurement, the river flow velocity (v_n) is about 3.56 m/s. In general, normal discharge in the study area is observed to vary from 333.60 m³/s to 387.80 m³/s. Furthermore, after normal and rational discharges are estimated; total discharge in the study area can be obtained.

Table 4 presents summary of the critical river water level and normal water level based on the accumulation rational and normal discharge. In Table 4, it can be seen that the critical river water level in the estuary area is observed to vary from 3.62 to 4.03 m. Therefore, it can be concluded that the rainfall could result in the increase of river water level of about 0.84 to 1.03 m. Based on the results, finite element analysis considering the change of river water level is conducted. The result of the analysis is presented in the next section.

.

Monthly Rainfall Intensity for Period of 2011-2020
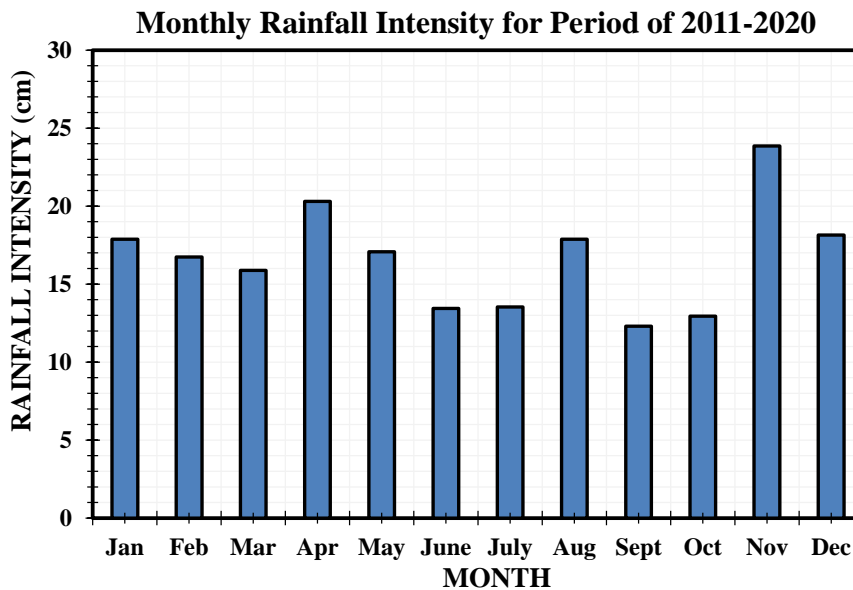
Fig. 5. Monthly rainfall [37].

Table 2. Summary of rational discharge.

Cross Section	Coefficient of Runoff	Rainfall Intensity	Section Area	Rational Discharge
	(C)	I (cm)	(A) (km²)	(Q_{rat}) (m³/s)
MK-1 and MK-2	0.6	16.66	0.13	314.37
MK-3 and MK-4	0.6	16.66	0.16	313.74
MK-5 and MK-6	0.6	16.66	0.22	269.51
MK-7 and MK-8	0.6	16.66	0.18	281.27
MK-9 and MK-10	0.6	16.66	0.16	281.79

Table 3. Summary of normal discharge.

Cross Section	Normal River Flow	w_{n1}	w_{n2}	h_n	Normal Discharge
	(v_n) m/s	(m)	(m)	(m)	(Q_n) (m³/s)
MK-1 and MK-2	3.56	36.60	36.00	3.00	387.68
MK-3 and MK-4	3.56	37.75	34.70	2.99	385.59
MK-5 and MK-6	3.56	33.55	31.30	2.89	333.60
MK-7 and MK-8	3.56	38.40	38.40	2.78	380.04
MK-9 and MK-10	3.56	37.00	36.10	2.74	356.52

Table 4. Summary of total discharge and critical river water level (h_f).

Cross Section	Flood River Flow	w_f	w_{n2}	Total Discharge	h_f
	(v_f)	(m)	(m)	(Q_{total}) (m³/s)	(m)
MK-1 and MK-2	4.76	37.20	36.00	702.05	4.03
MK-3 and MK-4	4.76	40.80	34.70	699.33	3.89
MK-5 and MK-6	4.76	35.80	31.30	603.11	3.78
MK-7 and MK-8	4.76	38.40	38.40	661.31	3.62
MK-9 and MK-10	4.76	37.90	36.10	638.32	3.62

3.2. Slope Stability Analysis Results

The results of finite element simulation for slope stability analysis are presented in Figs. (6) to (9). In this study, some slopes that are assumed as the representative slopes. They are MK-2, MK-6, and MK-9. MK-2, MK-6, and MK-9 represent the front-side segment slope, middle-side segment slope, and back-side segment slope, respectively. Figures 6 and 7 showed the mesh deformation under both normal and critical conditions. It can be seen that the deformation is generally started at slope toe. It indicates that the slope tends to undergo sliding starting at slope toe. Generally, both conditions showed that failure surface could occur along the slope body. To observe the sliding planes on the investigated slopes, the sliding surfaces on three representative slopes are presented in Figures 8 and 9. In general, it can be observed that there is no significant difference between normal condition and critical condition. The sliding surface is generally occurred at the slope body. It indicates that both conditions could influence slope stability in the study area.

Table 5 presents the summary of FS under both normal and critical conditions and the percentage of FS difference between normal and critical conditions. In Table 5, it can be seen that there is a reduction of FS at each investigated slope due to the effect of river water level change under normal and critical conditions. Table 5 also presents that the reduction of FS between both conditions is not very significant. This is due to the fact that the slope has been getting saturated before the increase of river water level. During the increase of pore water pressure, FS values decrease [39]. Several studies conducted by Sun *et al.* [40], Xiong *et al.* [41] mentioned that due to the increase of river water level, the shear strength is reduced; therefore, FS is also decreased [42]. Based on Table 5, the difference percentage on the factor of safety reduction between normal and critical conditions is observed to vary from 0.88% to 6.45%. The results also present that factor of safety (FS) under both conditions show the unstable tendency. This is because

FS on each slope is less than 1.5. Therefore, it can be roughly estimated that the slope failure potentially happens in Muaro Kualo Segment. It can be concluded that the increase of river water level could influence the slope stability in the study area.

Table 6 presents the summary of total displacement on each slope, under both normal and critical conditions. It can be seen that under normal condition, the displacement is observed to vary from 0.81 to 2.26 m. For critical condition, it can be observed that under the critical condition, the total displacement is observed to vary from 1.22 to 1.88 m. This is due to the fact that slope has been getting saturated before the increase of river water level. However, in terms of total displacement, the critical condition tends to yield larger values than normal condition. Generally, the percentage of total displacement difference under both normal and critical conditions is observed to vary from 7.41 to 88.4%. The larger displacement could be resulted by the overflowing of riverbank slope due to the increase of river water level [43]. In the link to Figs. 8 and 9, it can be observed that the maximum displacement is generally occurred at the slope body; whereas Figs. 6 and 7 show the extreme displacement occurred at slope toe. It indicates that there is the accumulation of shear strength reduction due the increase of pore water pressure resulted from the increase of river water level. Several studies conducted by Gill *et al.* [44], Sobhanmanesh *et al.* [45], Bushira *et al.* [46] also show the similar trend of displacement. Singh *et al.* [47] mentioned that the extreme displacement at slope toe indicates the slope tends to be more vulnerable to fail down. Therefore, it can be roughly predicted that the slope failure in the riverbank slope is initiate by the shear strength reduction at slope toe.

3.3. Slope Vulnerability Maps

In this study, combination between Krigging and Gridding interpolating methods [36] is implemented to compose maps of slope vulnerability in the study area.

This method is commonly implemented by several researchers [48-50] to compose hazard maps in an area.

Figure 10 presents the zone distribution of slope vulnerability based on factor of safety, for Muaro Kualo Segment. As presented in Section 3.2, FS at each investigated site presents value less than 1.5. This threshold is used as the parameter to define the stability of slope. Therefore, under both normal and critical conditions, it can be observed that the investigated locations can be categorised as the vulnerable area to undergo slope failure during the effect of river water level change.
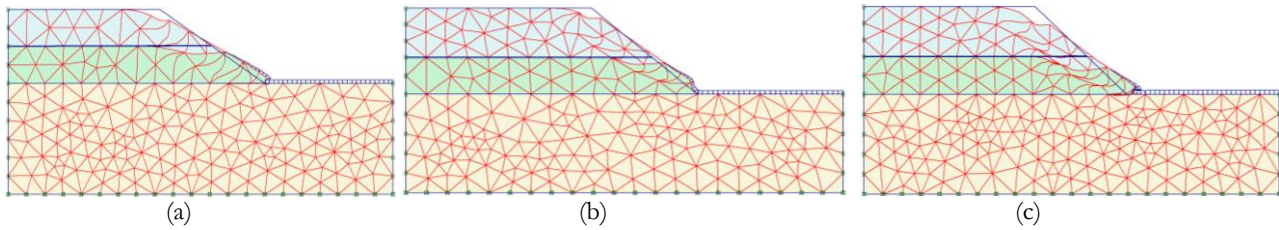
Fig. 6. Mesh deformation slope under normal condition at (a) MK-2 (b) MK-6 and (c) MK-9.
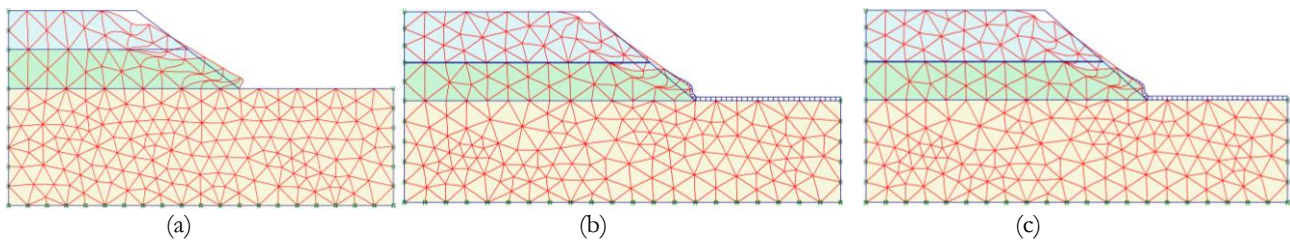
Fig. 7. Mesh deformation slope under critical condition at (a) MK-2 (b) MK-6 and (c) MK-9
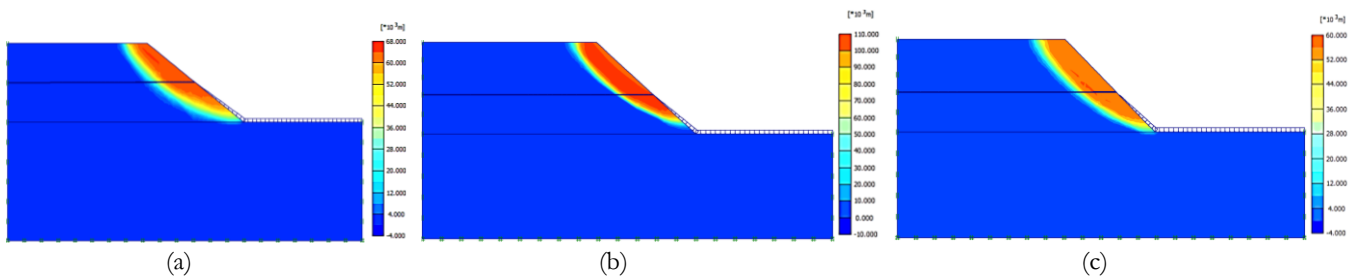
Fig. 8. Sliding surface slope under normal condition at (a) MK-2 (b) MK-6 and (c) MK-9.
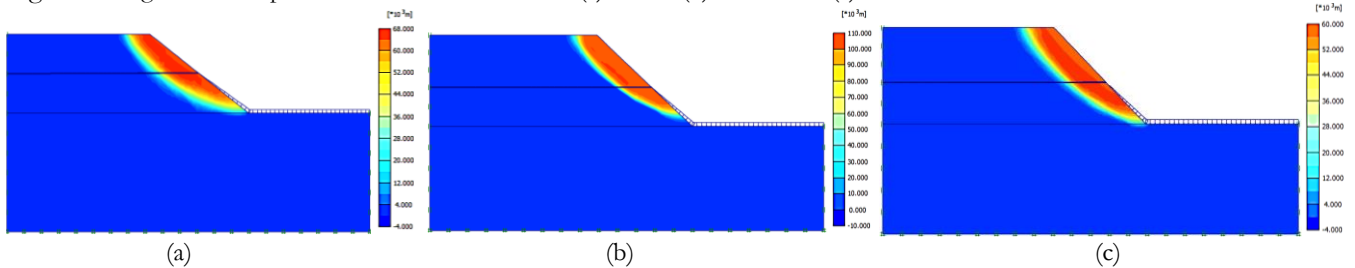
Fig. 9. Sliding surface slope under critical condition at (a) MK-2 (b) MK-6 and (c) MK-9.

Table 5. Summary of FS and percentage of FS difference under normal and critical condition.

Slopes	Coordinates		Factor of Safety (FS)		Percentage of FS Difference (%)
	Latitude	Longitude	Normal Condition	Critical Condition	
MK-1	102°15'54.07"E	3°46'23.37"S	1.35	1.33	1.48
MK-2	102°15'46.45"E	3°46'24.24"S	1.24	1.16	6.45
MK-3	102°15'56.13"E	3°46'36.47"S	1.07	1.06	0.93
MK-4	102°15'51.11"E	3°46'38.98"S	1.46	1.44	1.37
MK-5	102°16'02.76"E	3°46'39.45"S	1.08	1.07	0.93
MK-6	102°16'02.49"E	3°46'43.77"S	1.11	1.10	0.90
MK-7	102°16'13.90"E	3°46'42.05"S	1.09	1.08	0.92
MK-8	102°16'09.37"E	3°46'45.63"S	1.34	1.32	1.49
MK-9	102°16'21.88"E	3°46'50.76"S	1.13	1.12	0.88
MK-10	102°16'18.41"E	3°46'54.27"S	1.00	0.99	1.00

Table 6. Summary of total displacement under normal and critical condition.

Slopes	Coordinates		Total Displacement (m)		Percentage of Displacement Difference (%)
	Latitude	Longitude	Normal Condition	Critical Condition	
MK-1	102°15'54.07"E	3°46'23.37"S	0.81	1.53	88.64
MK-2	102°15'46.45"E	3°46'24.24"S	1.30	1.65	27.31
MK-3	102°15'56.13"E	3°46'36.47"S	1.31	1.88	44.18
MK-4	102°15'51.11"E	3°46'38.98"S	1.39	1.49	7.41
MK-5	102°16'02.76"E	3°46'39.45"S	2.26	1.08	52.07
MK-6	102°16'02.49"E	3°46'43.77"S	1.11	1.22	10.44
MK-7	102°16'13.90"E	3°46'42.05"S	2.28	1.31	42.57
MK-8	102°16'09.37"E	3°46'45.63"S	1.44	1.53	6.25
MK-9	102°16'21.88"E	3°46'50.76"S	2.52	1.72	31.75
MK-10	102°16'18.41"E	3°46'54.27"S	2.20	1.48	32.73

Figure 11 presents the zone of slope displacement for Muaro Kualo under normal and critical conditions. For normal condition (Fig. 11(a)), it can be seen that the area in northern segment part is generally dominated by displacement varying from 1 to 1.5 m. For eastern to southern segment parts, the displacement is generally observed to vary from 2 to 2.5 m. In the middle part of segment, the displacement is generally observed to vary from 1.5 to 2 m. For critical condition (Fig. 11(b)), the displacement on the northern and southern segment parts is about 1.5 to 1.75 m, whereas the displacement on the middle part of segment part is observed to vary from 1.25 to 1.5 m. In general, there is no significant difference on the displacement zonation under both conditions. This is due to the fact that under both conditions, slopes on Muaro Kualo Segment have been potentially failure. The results of this study could recommend slope countermeasure for study area.

3.4. Slope Countermeasure Effort

Muaro Kualo is known as the port area that is very important to support socio-economic sector in Bengkulu City. However, the effect of flood during last 10 years has significantly influenced the riverbank slope. Figure 12 presents evidence of slope failure after the Bengkulu flood in April 2019. Figure 12(a) shows a massive slope failure at MK-2 and Fig. 12(b) shows the scouring effect at MK-9 due to the river stream during the flood. Based on the evidence, it can be seen that the slope damage is not only coming from the increase of river water level but also the high-speed of river stream scouring slope body along the segment. A slope countermeasure effort has been currently implemented to the segment. The slope countermeasure method implemented to the riverbank slope of Muaro Kualo Segment is the application of concrete sheet piles, especially at the port area, as presented in Fig. 13. In Fig. 13(a), it can be seen that the concrete sheet piles are installed at the slope toe of estuary riverbank. The construction of sheet pile is inserted to the slope toe and at the gap between the sheet pile and the top of slope is constructed as the new port for Muaro Kualo segment (Fig. 13(b))

A finite element analysis to the existing slope countermeasure is performed. Figure 14 presents the results of finite element analysis for the implementation of slope countermeasure effort. The slope countermeasure is conducted by installing concrete sheet piles with the buried length of about 4 m and the free length of about 4 m. In this study, axial stiffness (EA), bending stiffness (EI), plate thickness (d) and Poisson's ratio are assumed to be 3,250,000 kN/m², 28,600 kN/m², 0.325 m and 0.15, respectively. The model material is assumed as linear elastic model. For the space between the sheet pile and top of slope, the backfill material is compacted. At the top of sheet piles, a concrete plate is constructed as the pier. In general, the use of sheet pile is destined to avoid overflowing of river water and to avoid infiltration of river water to slope toe. In terms of erosion of soil due to river stream, sheet pile is also addressed to avoid the scouring effect. In analysis, step of construction is performed. the pile is initially installed and loading is applied. In this study, the surcharge load is acted behind sheet pile. Based on Fig. (14), it can be seen that during the critical condition, the failure surface generally occurs at the top of sheet pile (Fig. 14(a)). The maximum displacement is presented in Fig. 14(b). The maximum displacement occurred is located behind the sheet pile, which is the interface zone between load and sheet pile. FS under the condition is about 1.64. In general, FS of the slope countermeasure has been exceeded the minimum required FS. Therefore, the implementation of sheet piles as slope countermeasure effort for study area is relevant and reliable to the condition on the estuary area.
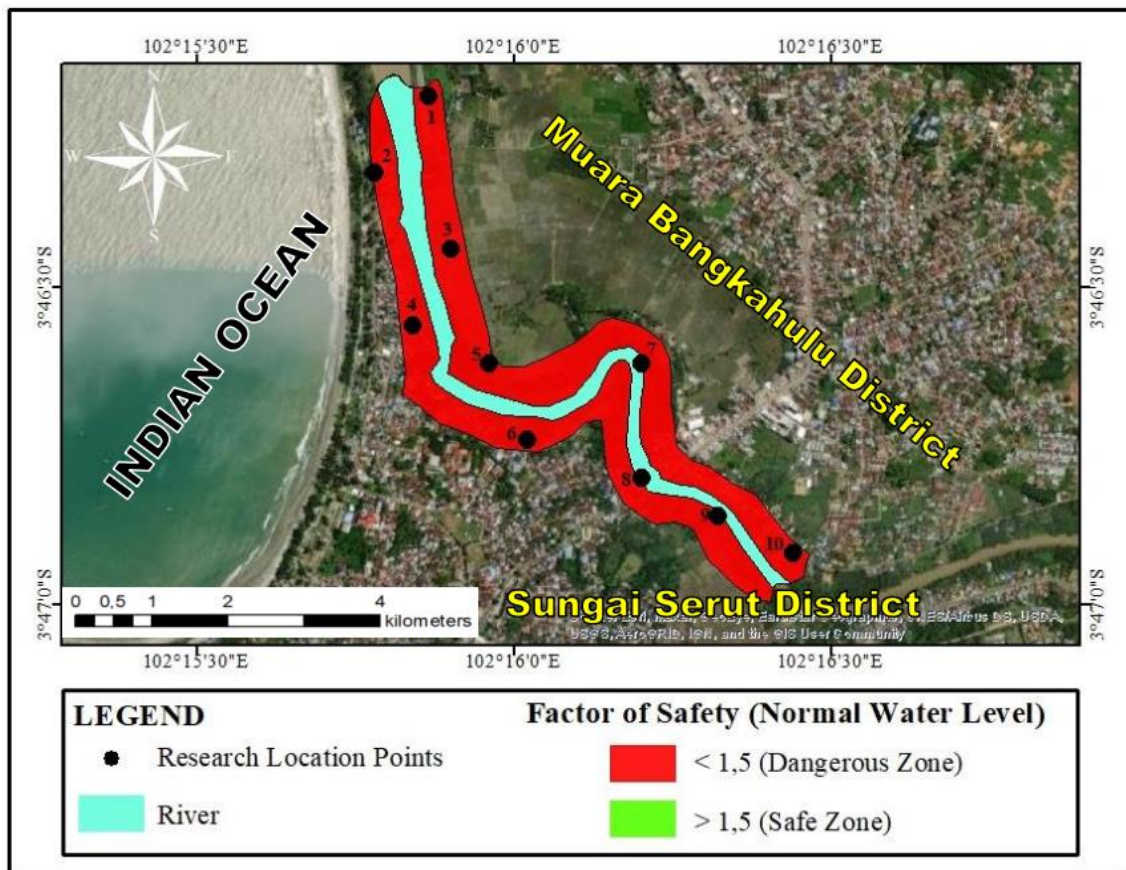
(a)
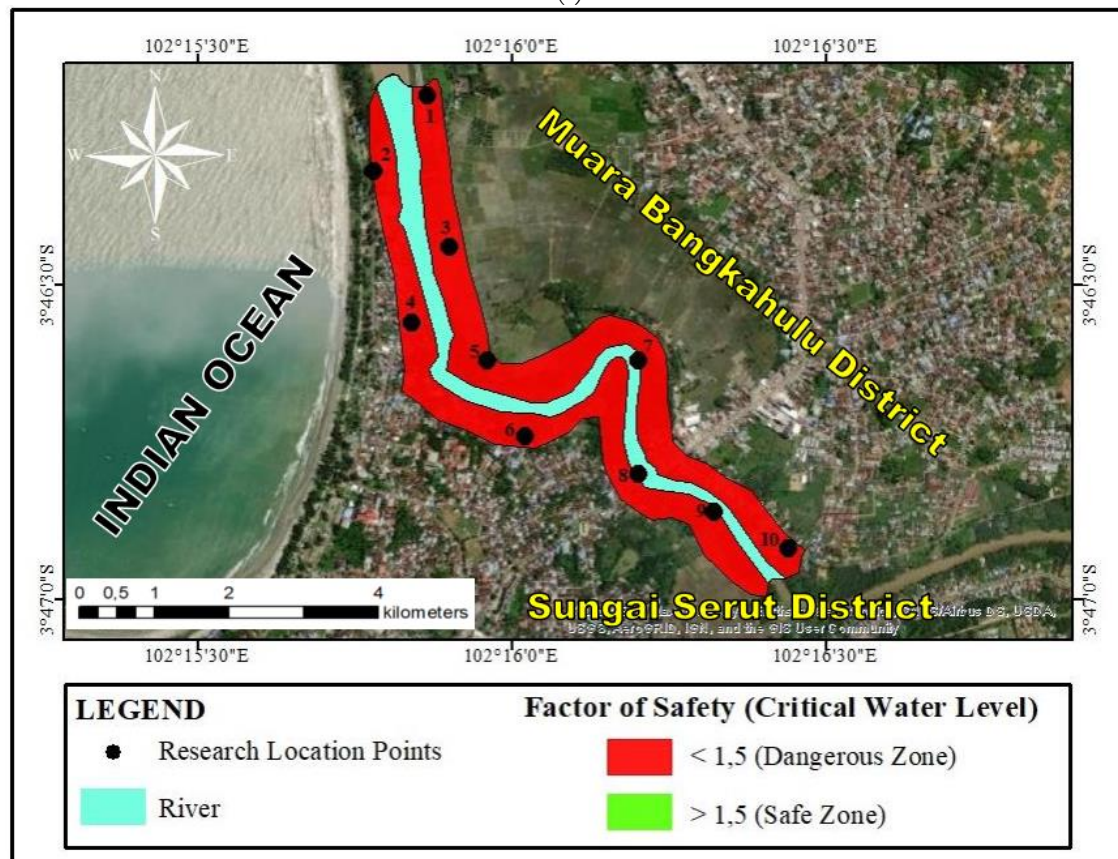
(b)

Fig. 10. Zones of slope vulnerability (basic map modified from Google Earth [12]) for Muaro Kualo Segment under (a) normal condition; (b) critical condition.
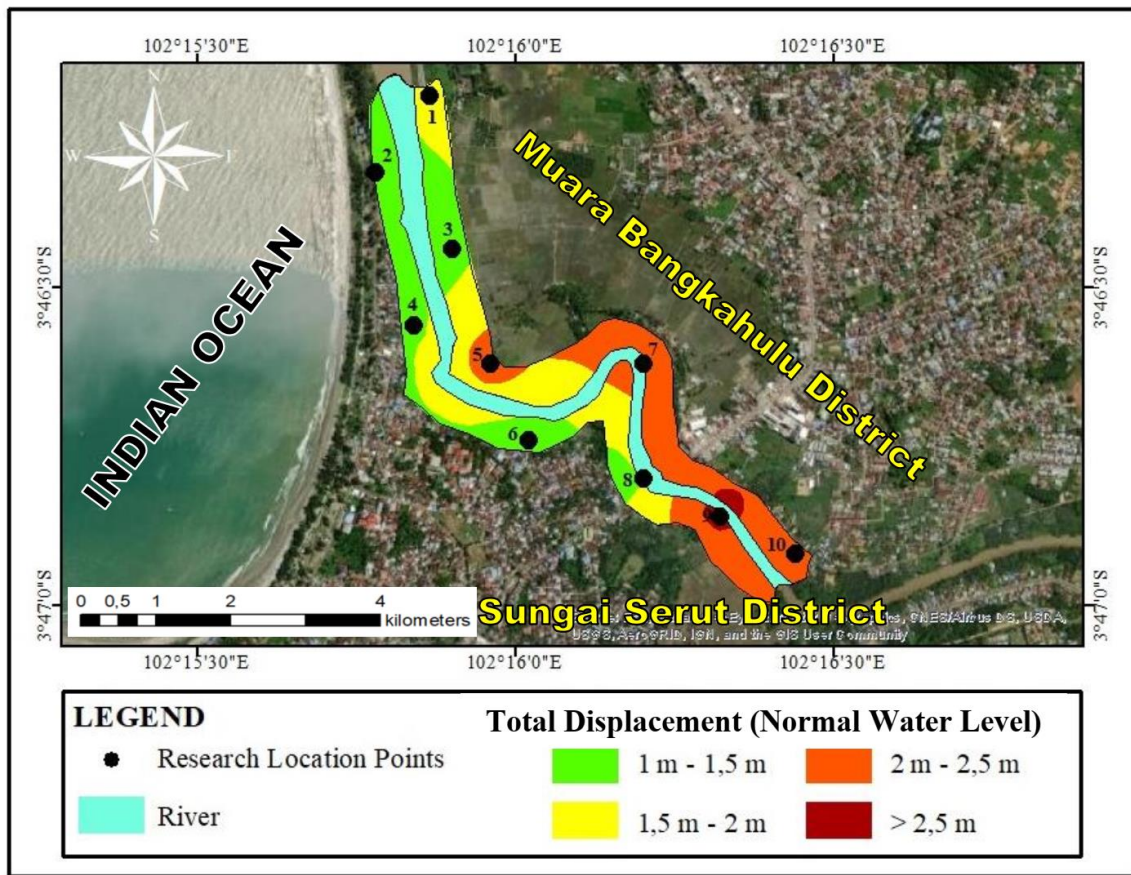
(a)
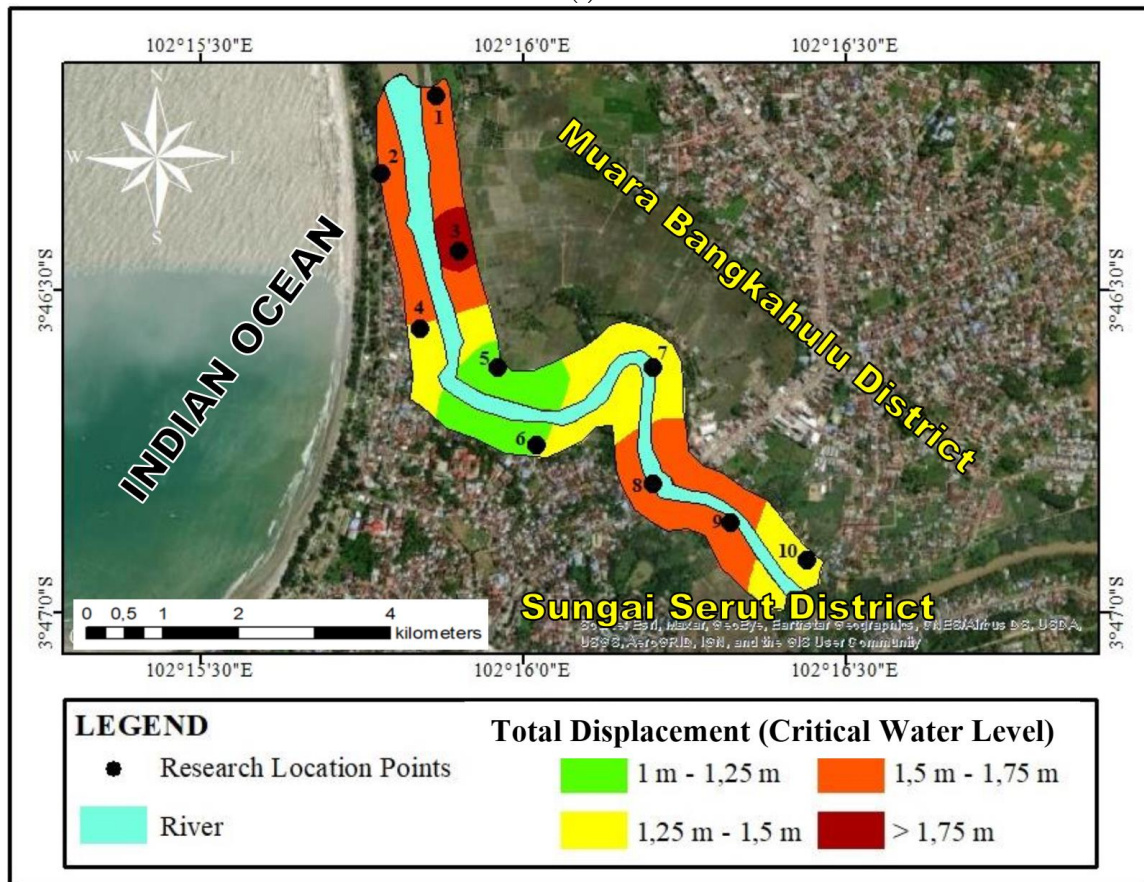
(b)

Fig. 11. Zones of total displacement (basic map modified from Google Earth [12]) for Muaro Kualo Segment under (a) normal condition; (b) critical condition.

(a)   (b)

Fig. 12. Slope damage due the Bengkulu Flood in April 2019 (a) slope failure at MK-3; (b) scouring slope at MK-7.

(a)   (b)

Fig. 13. Slope countermeasure at port area of Muaro Kualo Segment (a) the implementation of sheet pile; (b) top view of port area.
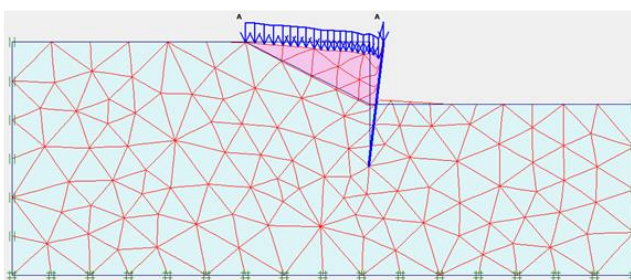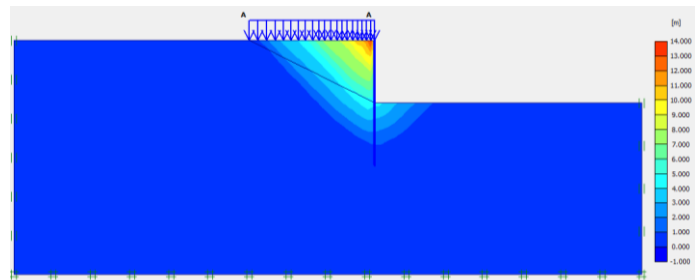
(a)   (b)

Fig. 14. Finite element results for slope countermeasure effort (a) mesh deformation; (b) sliding surface.

4. Conclusion

This paper presents the study of the effect of river water level fluctuation to riverbank slope stability at the Estuary Area of Muaro Kualo Segment, Muara Bangkahulu River, Bengkulu, Indonesia. The hydrological analysis to estimate the increase of river water level is conducted. Finite element analysis is conducted to observe the effect of water level fluctuation on slope stability. The slope vulnerability maps are composed based on the results of finite element. The implementation of slope countermeasure to the study area is also presented. Several concluding remarks can be drawn:

1. Site investigation and laboratory test are conducted to investigate soil characteristic. In general, sandy soils are dominantly found in the study area. Sandy soils in the study area are generally found at the riverbank slope. This material is relatively loose and easily to be scoured due to the river stream.
2. This study proposes the method to estimate the increase of river water level considering the period of

10 years based on the discharge analysis. The combined method between rational discharge and normal discharge analyses could be implemented to estimate the critical river water level, which is used to predict the effect of river water fluctuation at the riverbank slope. This proposed method is reasonably implemented to investigate similar cases.

3. The finite element analysis to both normal and critical conditions shows that there is generally no significant difference on factor of safety values between normal and critical conditions. Under the normal condition, riverbank slope has been already unstable. Once the increase of river water level, the riverbank slope becomes more unstable and more vulnerable to collapse. Therefore, it can be concluded that the increase of river water level is placing the slope to be getting more vulnerable. Slope vulnerability maps composed from this study are also useful to depict the potential slope failure hazard in the study area.

4. The slope countermeasure by using concrete sheet pile is selected to solve the problem of slope failure in the study area. In general, the implementation of slope countermeasure method significantly improves slope stability in the study area up to 1.64. The slope countermeasure could significantly reduce the effect of overflowing of river water level, increase the slope stability, and reduce the scouring potential. The slope countermeasure implementation could maintain the function of old port of Bengkulu city to support the socio-economic aspect in Muaro Kualo Segment.

5. The study area is also the part of old-city of Bengkulu, which is known as the heritage of Bengkulu. In line with this, the result of this study could be a recommendation to the local government to improve the slope stability in the study area.

Acknowledgement

References

[1] M. Farid and L. Z. Mase, "Implementation of seismic hazard mitigation on the basis of ground shear strain indicator for spatial plan of Bengkulu City, Indonesia," *International Journal of Geomate*, vol. 18, no. 69, pp. 199-207, 2018.

[2] G. Mulyasari, L. R. Waluyati, and A. Suryantini, "Perceptions and local adaptation strategies to climate change of marine capture fishermen in Bengkulu Province, Indonesia," *IOP Conference Series. Earth and Environmental Science*, vol. 200, no. 1, p. 012037, 2020.

[3] L. Z. Mase, "Slope stability and erosion-sedimentation analyses along sub-watershed of Muara Bangkahulu River in Bengkulu City, Indonesia" *E3S Web of Conferences*, vol. 148, p. 03002, 2020.

[4] L. Z. Mase, A. Perdana, Hardiansyah, K. Amri and S. Bahri, "A case study of slope stability improvement in Central Bengkulu Landslide in Indonesia," *Transportation Infrastructure Geotechnology*, pp. 1-25. 2021.

[5] V. Komolvilas, W. Tanapalungkorn, P. Latcharote, and Likitlersuang, "Failure analysis on a heavy rainfall-induced landslide in Huay Khab Mountain in Northern Thailand," *Journal of Mountain Science*, vol. 18, no. 10, pp. 2580-2596, 2021.

[6] P. Jamsawang, P. Voottipruex, P. Jongpradist, and S. Likitlersuang, "Field and three-dimensional finite element investigations of the failure cause and rehabilitation of a composite soil-cement retaining wall," *Engineering Failure Analysis*, vol. 127, no. 9, p. 105532, 2021.

[7] U. Leknoi and S. Likitlersuang, "Good practice and lesson learned in promoting vetiver as solution for slope stabilisation and erosion control in Thailand," *Land Use Policy*, vol. 99, no. 12, p. 05008, 2020.

[8] T. T. Duong, H. Komine, M. D. Do, and S. Murakami, "Riverbank stability assessment under flooding conditions in the Red River of Hanoi, Vietnam," *Computers and Geotechnics*, no. 61, pp. 178-189, 2014.

[9] T. D. Thi and D. D. Minh, "Riverbank stability assessment under river water level changes and hydraulic erosion," *Water*, vol. 11, no. 12, p. 2598, 2019.

[10] C. Liang, M. B. Jaksa, B. Ostendorf, and Y. L. Kuo, "Influence of river level fluctuations and climate on riverbank stability," *Computers and Geotechnics*, vol. 63, pp. 83-98, 2015.

[11] A. Udomchai, M. Hoy, S. Horpibulsuk, A. Chinkulkijniwat, and A. Arulrajah, "Failure of riverbank protection structure and remedial approach: A case study in Suraburi province, Thailand," *Engineering Failure Analysis*, vol. 91, pp. 243-254, 2018.

[12] Google Earth. "Estuary Zone of Muara Bangkahulu River of Bengkulu City." Google Earth. https:// earth.google.com/web/search/Bengkulu/@-3.76433345,102.26378829,2.20577879a,2536.4 9306002d,35y,-0h,0t,0r/data=CigiJgokCb6orLUsR zRAEbyorLUsRzTAGd9wxF1rX0VAISRrskksiU3 A (accessed Feb. 2, 2022).

[13] J. M. Moreno-Maroto, J. Alonso-Azcárate, and B. C. O'Kelly, "Review and critical examination of fine-grained soil classification systems based on plasticity," *Applied Clay Science*, vol. 200, p. 105955, 2021.

[14] L. Z. Mase, Refrizon, Rosiana, and P. W. Anggraini, "Local site investigation and ground response analysis on downstream area of Muara Bangkahulu River, Bengkulu City, Indonesia," *Indian Geotechnical Journal*, pp. 1-15, 2021.

[15] J. E. Bowles, *Foundation Analysis and Design*, 5th ed. New York: McGraw-Hill, 1996.

[16] K. S. Cha and T. H. Kim, "Evaluation of slope stability with topography and slope stability analysis method," *KSCE Journal of Civil Engineering*, vol. 15, no. 2, pp. 251-256, 2011.

[17] R. B. J. Brinkgreve, W. M. Swolfs, and E. Engin, *PLAXIS User's Manual*. Delft: PLAXIS, 2011.

[18] S. Likitlersuang, C. Surarak, D. Wanatowski, E. Oh, and A. S. Balasubramaniam, "Finite element analysis of a deep excavation: A case study from the Bangkok MRT," *Soils and Foundations*, vol. 53, no. 5, pp. 756-773, 2013.

[19] S. Likitlersuang, C. Surarak, S. Suwansawat, D. Wanatowski, E. Oh, and A. S. Balasubramaniam, "Simplified finite-element modelling for tunnelling-induced settlements," *Geotechnical Research*, vol. 1, no. 4, pp. 133 – 152, 2014.

[20] R. Sukkarak, S. Likitlersuang, P. Jongpradist, and P. Jamsawang, "Strength and stiffness parameters for hardening soil model of rockfill materials," *Soils and Foundations*, vol. 61, no. 6, pp. 1597-1614, 2021.

[21] S. Keawsawasvong, C. Thongchom, and S. Likitlersuang, "Bearing capacity of strip footing on Hoek-Brown rock mass subjected to eccentric and inclined loading," *Transportation Infrastructure Geotechnology*, vol. 8, no. 2, pp. 189-202, 2021.

[22] S. Likitlersuang, C. Chheng, and S. Keawsawasvong, "Structural modelling in finite element analysis of deep excavation," *Journal of GeoEngineering*, vol. 14, no. 3, pp. 121-128, 2019.

[23] B. Ukritchon, S. Keawsawasvong, and K. Yingchaloenkitkhajorn, "Undrained face stability of tunnels in Bangkok Subsoils," *International Journal of Geotechnical Engineering*, vol. 11, no. 3, pp. 262-277, 2017.

[24] T. Matsui and K. C. San, "Finite element slope stability analysis by shear strength reduction technique," *Soils and Foundations*, vol. 32, no. 1, pp. 59-70, 1992.

[25] E. M. Dawson, W. H. Roth and A. Drescher, "Slope stability analysis by strength reduction," *Geotechnique*, vol. 49, no. 6, pp. 835-840, 1999.

[26] Q. Zhang, S. Wang, G. E. Xiurun, and H. Wang, "Modified Mohr-Coulomb strength criterion considering rock mass intrinsic material strength factorization," *Mining Science and Technology (China)*, vol. 20, no. 5, pp. 701-706, 2010.

[27] L. Z. Mase, S. Likitlersuang, and T. Tobita, "Cyclic behaviour and liquefaction resistance of Izumio sands in Osaka, Japan," *Marine Georesources & Geotechnology*, vol. 37, no. 7, pp. 765-774, 2019.

[28] A. P. Dyson and A. Tolooiyan, "Optimisation of strength reduction finite element method codes for slope stability analysis," *Innovative Infrastructure Solutions*, vol. 3, no. 1, pp. 1-12, 2018.

[29] L. Zhao, F. Yang, Y. Zhang, H. Dan, and W. Liu, "Effects of shear strength reduction strategies on safety factor of homogeneous slope based on a general nonlinear failure criterion," *Computers and Geotechnics*, vol. 63, no. 1, pp. 215-228, 2015.

[30] M. R. Arvin, A. Zakeri, and M. B. Shoorijeh, "Using finite element strength reduction method for stability analysis of geocell-reinforced slopes," *Geotechnical and Geological Engineering*, vol. 37, no. 3, pp. 1453-1467, 2019.

[31] G. You, M. A. Mandalawi, A. Soliman, K. Dowling, and P. Dahlhaus, "Finite element analysis of rock slope stability using shear strength reduction method," in *Soil Testing, Soil Stability and Ground Improvement. GeoMEast*, 2017. *Sustainable Civil Infrastructures.*, W. Frikha, S. Varaksin, A. Viana da Fonseca, Eds. Springer, Cham., 2018, pp. 227-235.

[32] K. Leelarungroj, S. Likitlersuang, T. Chompoorat, and D. Janjaroen, "Leaching mechanisms of heavy metals from fly ash stabilised soils" *Waste Management & Research*, vol. 36, no. 7, pp. 616-623, 2018.

[33] T. Chompoorat, K. Thanawong, and S. Likitlersuang, "Swell-shrink behaviour of cement with fly ash-stabilised lakebed sediment," *Bulletin of Engineering Geology and the Environment*, vol. 80, no. 3, pp. 2617-2628, 2021.

[34] B. Punnoi, S. Arpajirakul, W. Pungrasmi, T. Chompoorat, and S. Likitlersuang, "Use of microbially induced calcite precipitation for soil improvement in compacted clays," *International Journal of Geosynthetics and Ground Engineering*, vol. 7, no. 4, p. 86, 2021.

[35] T. F. Stark and D. G. Ruffing, "Selecting minimum factors of safety for 3D slope stability analyses," in *Geo-Risk 2017: Reliability-Based Design and Code Developments*, J. Huang, G. A. Fenton, L. Zhang, and D. V. Griffiths, Eds. ASCE, 2017, pp. 259-266.

[36] Q. Meng, Z. Liu, and B. E. Borders, "Assessment of regression kriging for spatial interpolation–comparisons of seven GIS interpolation methods," *Cartography and Geographic Information Science*, vol. 40, no. 1, pp. 28-39. 2013.

[37] River Territory Office (RTO), "Rainfall intensity in Muaro Kualo Area within 2011-2020," River Territory Office, Bengkulu, Indonesia, 2020.

[38] R. H. McCuen, *Hydrologic Analysis and Design*. New Jersey: Prentice Hall, 1989, p. 888.

[39] C. Kristo, H. Rahardjo, and A. Satyanaga, "Effect of variations in rainfall intensity on slope stability in Singapore," *International Soil and Water Conservation Research*, vol. 5, no. 4, pp. 258-264, 2017.

[40] G. Sun, Y. Yang, S. Cheng, and H. Zheng, "Phreatic line calculation and stability analysis of slopes under the combined effect of reservoir water level fluctuations and rainfall," *Canadian Geotechnical Journal*, vol. 54, no. 5, pp. 631-645, 2017.

[41] X. Xiong, Z. Shi, Y. Xiong, M. Peng, X. Ma, and F. Zhang, "Unsaturated slope stability around the Three Gorges Reservoir under various combinations of rainfall and water level fluctuation," *Engineering Geology*, no. 261, p. 105231, 2019.

[42] R. H. Latief and A. K. E. Zainal, "Effects of water table level on slope stability and construction cost of highway embankment," *Engineering Journal*, vol. 23, no. 5, pp. 1-12, 2019.

[43] F. Oka, S. Kimoto, R. Kato, S. Sunami, and T. Kodaka, "A soil-water coupled analysis of the deformation of an unsaturated river embankment due to seepage flow and overflow," in *Proc. of the 12th International Conference of International Association for Computer Methods and Advances in Geomechanics (IACMAG)*, M. N. Jadhav, Ed. Curran, 2008, no. 2029-2041, p. 4871.

[44] K. S. Gill, A. K. Choudhary, J. N. Jha, and S. K. Shukla, "Experimental and numerical studies of loaded strip footing resting on reinforced fly ash slope," *Geosynthetics International*, vol. 20, no. 1, pp. 13-25, 2013.

[45] A. Sobhanmanesh, R. Nazir, and N. Saadatkhah, "Effect of weathered surface crust layer on stability of Muar trial embankment," *Jurnal Teknologi*, vol. 76, no. 2, pp. 31-38, 2015.

[46] K. M. Bushira, Y. B. Gebregiorgis, R. K. Verma, and Z. Sheng, "Cut soil slope stability analysis along national Highway at wozeka–gidole road, Ethiopia," *Modeling Earth Systems and Environment*, vol. 4, no. 2, pp. 591-600, 2018.

[47] R. Singh, R. K. Umrao, and T. N. Singh, "Probabilistic analysis of slope in Amiyan landslide area, Uttarakhand," *Geomatics, Natural Hazards and Risk*, vol. 4, no. 1, pp. 13-29, 2013.

[48] I. N. Sinarta, A. Rifa'i, T. F. Fathani, and W. Wilopo, "Slope stability assessment using trigger parameters and SINMAP methods on Tamblingan-Buyan ancient mountain area in Buleleng Regency, Bali," *Geosciences*, vol. 7, no. 4, p. 110, 2017.

[49] S. Likitlersuang, P. Plengsiri, L. Z. Mase, and W. Tanapalungkorn, "Influence of spatial variability of ground on seismic response analysis: a case study of Bangkok subsoils," *Bulletin of Engineering Geology and the Environment*, vol. 79, no. 1, pp. 39-51, 2020.

[50] L. Z. Mase, N. Sugianto, and Refrizon, "Seismic hazard microzonation of Bengkulu City, Indonesia," *Geoenvironmental Disasters*, vol. 8, no. 1, pp. 1-17, 2021.

——— • ———

Lindung Zalbuin Mase, photograph and biography not available at the time of publication.

Khairul Amri, photograph and biography not available at the time of publication.

Muhammad Farid, photograph and biography not available at the time of publication.

Fandi Rahmat, photograph and biography not available at the time of publication.

Muharram Nur Fikri, photograph and biography not available at the time of publication.

Jihan Saputra, photograph and biography not available at the time of publication.

Suched Likitlersuang, photograph and biography not available at the time of publication.